Journal of Analytical and Applied Pyrolysis 170 (2023) 105900

Contents lists available at ScienceDirect

Journal of Analytical and Applied Pyrolysis

journal homepage: www.elsevier.com/locate/jaap

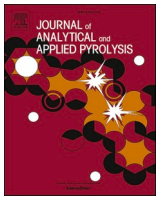

Effects of minerals (phyllosilicates and iron oxides) on the responses of aliphatic hydrocarbon containing kerogens (Type I and Type II) to analytical pyrolysis

Tara L. Salter *, Jonathan S. Watson, Mark A. Sephton

Department of Earth Science and Engineering, Imperial College London, UK

ARTICLE INFO

Keywords:
Pyrolysis-GC-MS
Kerogen
Phyllosilicates
Iron oxides
Polyethylene

ABSTRACT

Organic matter in sediments is dominated by kerogen, a high molecular weight geomacromolecule. Kerogen can be subdivided into Types I to IV that provide paleoenvironmental and petroleum potential information. Kerogen typing can be performed by several chemical methods including elemental analysis (H/C and O/C), FTIR and pyrolysis-gas chromatography techniques. However, kerogens occur naturally within mineral matrices and these can influence the chemical responses. We have examined the effects of a range of minerals (namely kaolinite, lizardite, ripidolite, illite, montmorillonite, haematite, goethite, limonite and magnetite) on the responses of kerogen to pyrolysis-gas chromatography-mass spectrometry. We used aliphatic hydrocarbon containing kerogen Types I and II from Carboniferous Midland Valley shales of Scotland and the Jurassic Oxford Clay of southern England, respectively, as well as a pure synthetic aliphatic polymer, polyethylene. We find that the aliphatic organic matter in Type I kerogens is transformed by interaction with minerals during pyrolysis to give a signal incorrectly suggesting more contributions from land plant-containing kerogens, such as a large number of aromatic molecules. Pyrolysis with goethite, limonite and magnetite leads to almost complete destruction of the organic matter. Hence, the mineral composition of sedimentary rocks during pyrolysis should be considered when assigning kerogen types. Failure to consider the effects of minerals can lead to incorrect assignment of kerogen type and, therefore, erroneous interpretations of paleoenvironments and petroleum potential.

1. Introduction

Kerogen is sedimentary organic matter that is insoluble in common organic solvents. Kerogen can be subdivided into four types, chemically defined by their hydrogen to carbon (H/C) and oxygen to carbon (O/C) ratios [1]. H/C ratios are influenced by the degree of unsaturation in the molecular architecture, while O/C ratios are controlled by the presence of oxygen containing functional groups. Type I kerogens have high H/C and low O/C ratios and are associated with algal organic matter. Type III kerogens have low H/C ratios and high O/C ratios and are associated with land plant material. Type II kerogens have intermediate H/C and O/C ratios reflecting mixed kerogens with both algae and land plant inputs. Type IV kerogens have very low H/C and high O/C ratios reflecting reworked and oxidised organic matter. All kerogen types progress to carbon-rich residues during thermal maturation. In this study, our focus was on the hydrogen-rich kerogen types (Type I and Type II) and their long carbon hydrocarbon chain contents. Kerogen types have been identified by other methods such as programmed pyrolysis, analytical pyrolysis and Fourier Transform infra-red spectroscopy (FTIR) [2–4]. The different analytic responses derived from the various kerogen types reflect the underlying chemical structure [5,6].

The presence of unsaturated bonds, in particular aromatic units, and oxygen containing groups can be recognised by spectroscopic techniques such as FTIR but also in the products of heating techniques such as analytical pyrolysis [4,7–9]. However, it has been known for some time that the products of pyrolysis are influenced by the mineral matrix in which any organic matter is hosted [10–13]. In fact, the influence of minerals on hydrocarbons during heating [14] has been exploited for decades allowing cracking of larger hydrocarbons to smaller products during petroleum refining.

The catalytic effect of phyllosilicates on the pyrolysis of organic samples has been studied previously [15–20]; this includes the clay minerals, kaolinite [21,22] and montmorillonite [12,23–25]. Montmorillonite is considered to be a very active matrix in terms of absorption of

* Corresponding author.
E-mail address: t.salter@imperial.ac.uk (T.L. Salter).

https://doi.org/10.1016/j.jaap.2023.105900
Received 3 November 2022; Received in revised form 16 December 2022; Accepted 31 January 2023
Available online 1 February 2023

products and its ability to crack organic matter [26]. The presence of montmorillonite has been found to enhance the formation of naphthalenes and phenanthrenes during the pyrolysis of Type II Cretaceous black shale [27]. Similarly, the relative abundance of polycyclic aromatic hydrocarbons was found to increase with mineral acidity when Kukersite kerogen was pyrolysed with the minerals, kaolinite, montmorillonite, calcite and dolomite [28]. Iron oxides have also been found to have catalytic properties [29], with increased amounts of small aromatic compounds (benzene, toluene, ethylbenzene, xylene and naphthalene) observed when limonite was used as a catalyst in the pyrolysis of a low-rank coal [30].

Here, we have examined the influence of minerals on the products of pyrolysis to assess whether standard interpretations of analytical pyrolysis can be affected by certain minerals. Analytical pyrolysis deals with the final combined organic and mineral assemblage found in rock samples. Hence, we have chosen minerals that are found as both primary phases in sedimentary deposits and secondary phases generated by alteration by weathering processes (e.g. oxides and oxyhydroxides). The phyllosilicates kaolinite, lizardite, ripidolite, illite and montmorillonite, and the iron (hydroxy)oxides magnetite, goethite, haematite, limonite, have all been investigated. For the kerogen samples we concentrated our efforts on those kerogens that have substantial amounts of hydrogen-rich aliphatic material derived from aliphatic biolpolymers, namely Type I and Type II kerogens. To constrain and therefore understand the mineral induced reactions in detail we also used a pure synthetic aliphatic polymer, polyethylene (PE). Our findings improve our appreciation of the complexity of interpreting the pyrolysis responses of organic materials in mineral matrices.

2. Methods

2.1. Samples

The West Lothian shale (Type I kerogen) was deposited in the Lower Carboniferous and was collected from Port Edgar, West of Craigs in Scotland. The Oxford Clay shale (Type II kerogen) is Callovian to Oxfordian age and was collected from Chickerell, Crook Hill Nature Reserve near Weymouth, south coast of England. Programmed pyrolysis (RockEval) data for the rock samples from which kerogen was isolated is presented in Table 1. These data indicate kerogen type.

Polyethylene was obtained in powder form (Sigma Aldrich). Na-rich montmorillonite (SWy-2), illite (IMt-1), ripidolite (CCa-2) and kaolinite (KGa-1b) were obtained from the Source Clay Repository of the Clay Minerals Society. Lizardite was collected from Kennack Sands beach, Lizard Peninsula, Cornwall, UK. Magnetite and goethite were obtained from Sigma-Aldrich. Haematite and limonite were sourced from the Imperial College ESE rock collection and were both collected in the Mendip Hills, UK.

All samples were ground to a powder using a pestle and mortar. Mixtures of organic material and clays were composed of 2% w/w organic material (kerogen or polyethylene) and 98% clay or iron oxide.

Table 1
Samples used in the pyrolysis-GC-MS study and their geochemical characteristics. TOC: total organic carbon (%); S1 (mg hydrocarbons/g rock): reflects free hydrocarbons (gas and oil) in the rock; S2 (mg hydrocarbons/g rock): reflects hydrocarbons liberating from kerogen cracking; S3 (mg CO_2/g rock): reflects CO_2 released from pyrolysis of kerogen and is an indication of oxygen in kerogen; T_{max} (°C): temperature at which S2 reaches a maximum and is an indicator of kerogen thermal maturity; HI: Hydrogen Index = [100 x S2]/TOC and is a practical equivalent to H/C, OI: Oxygen Index = [100 x S3]/TOC and is a programmed pyrolysis practical equivalent to O/C [35].

Name	TOC %	S1 mg/g	S2 mg/g	S3 mg/g	HI	OI	T_{max} °C
Port Edgar	19.90	3.54	145.93	0.84	733	4	450
Oxford Clay	11	0.67	46.28	9.42	421	86	416

2.2. Pyrolysis-gas chromatography-mass spectrometry

For pyrolysis experiments, samples were placed in quartz pyrolysis tubes plugged with quartz wool at each end. Pyrolysis-gas chromatography-mass spectrometry (pyrolysis-GC-MS) was performed using a 2000 Pyroprobe (CDS Analytical) fitted via a CDS 1500 valve interface. Samples were heated to 650 °C, at a rate of 20 °C ms^{-1}, and held there for 15 s, in a flow of helium. The pyrolysis unit was coupled to a 6890 gas chromatograph coupled to a 5973 mass spectrometer (both Agilent Technologies). The GC inlet was held at 270 °C. Separation was performed on a DB-5 ms ultra inert column (J&W; approximately 30 m x 0.25 mm × 0.25 μm), operated in split mode (10:1) with a helium column flow rate of 1.1 ml min^{-1}. The gas chromatograph oven was held at an initial temperature of 40 °C for 2 mins, then increased at a rate of 5 °C min^{-1} to reach a final temperature of 310 °C, which was held for 10 mins.

Mass spectra were acquired over the range 45–550 amu. Identification of peaks in the chromatograms was carried out using the Agilent MSD Chemstation software with comparison to the NIST mass spectral library, characterised samples, standards and custom libraries. At least two repeat experiments were performed for each sample analysed.

3. Results

3.1. Pyrolysis-GC-MS of polyethylene

To understand the effects of phyllosilicate minerals and iron oxides on the pyrolysis of organic samples, firstly pure organic samples were analysed. The top panel (a) of Fig. 1 shows the pyrolysis-GC-MS products of polyethylene (PE) alone. This figure shows that the pyrolysis of PE produces a repeating series of triplet peaks, consisting of *n*-dienes, *n*-alkenes and *n*-alkanes. The *n*-alkene peak is the largest of the three, with the *n*-diene and *n*-alkane peaks being of a similar size. *n*-alkenes were detected in the series C_6 to C_{33}, whereas alkanes and dienes were detected from C_8 to C_{33}.

A range of different mineral-induced effects were observed when PE (2% w/w) was pyrolyzed in the presence of phyllosilicate minerals and iron oxides. The panels b to f of Fig. 1 show the effects of the phyllosilicates, kaolinite, lizardite, ripidolite, illite and montmorillonite respectively, on the pyrolysis products of PE. All of the minerals used in these experiments changed the distribution of the compounds identified compared to PE on its own. PE pyrolysed with kaolinite, Fig. 1b, retains the alkene/alkane doublet which is reduced to the alkane component at higher retention times, approximately C_{21}. The alkane/alkene distribution was also skewed towards the shorter chain lengths. Branched chain hydrocarbons were also observed at the lower retention times. The *n*-alkane component was observed to varying extents in the PE samples mixed with lizardite, illite and ripidolite, Fig. 1c-e. However, this was reduced to a minor component compared to the relatively large intensity of aromatic molecules observed, namely toluene and alkylbenzenes. Methylnaphthalenes were also observed in the PE and illite mixed sample.

In contrast to the other samples, only a tiny amount of the aliphatic hydrocarbon signal remains in the PE and montmorillonite mixed sample. Instead, alkylbenzenes dominate the total ion chromatogram (TIC), shown in Fig. 1f. Alkylnaphthalenes were also detected at higher retention times.

The panels g to j of Fig. 1 show the pyrolysis products of PE mixed with the iron oxides, haematite (Fe(III) oxide), goethite (Fe(III) oxyhydroxide), limonite and magnetite (Fe(II,III) oxide). It can clearly be seen that iron oxides affect the analysis of PE, with very little of the original pyrolysis products retained. The TICs of PE mixed with haematite, goethite and limonite are similar, with some of the original hydrocarbon alkane/alkene background of PE remaining, however this

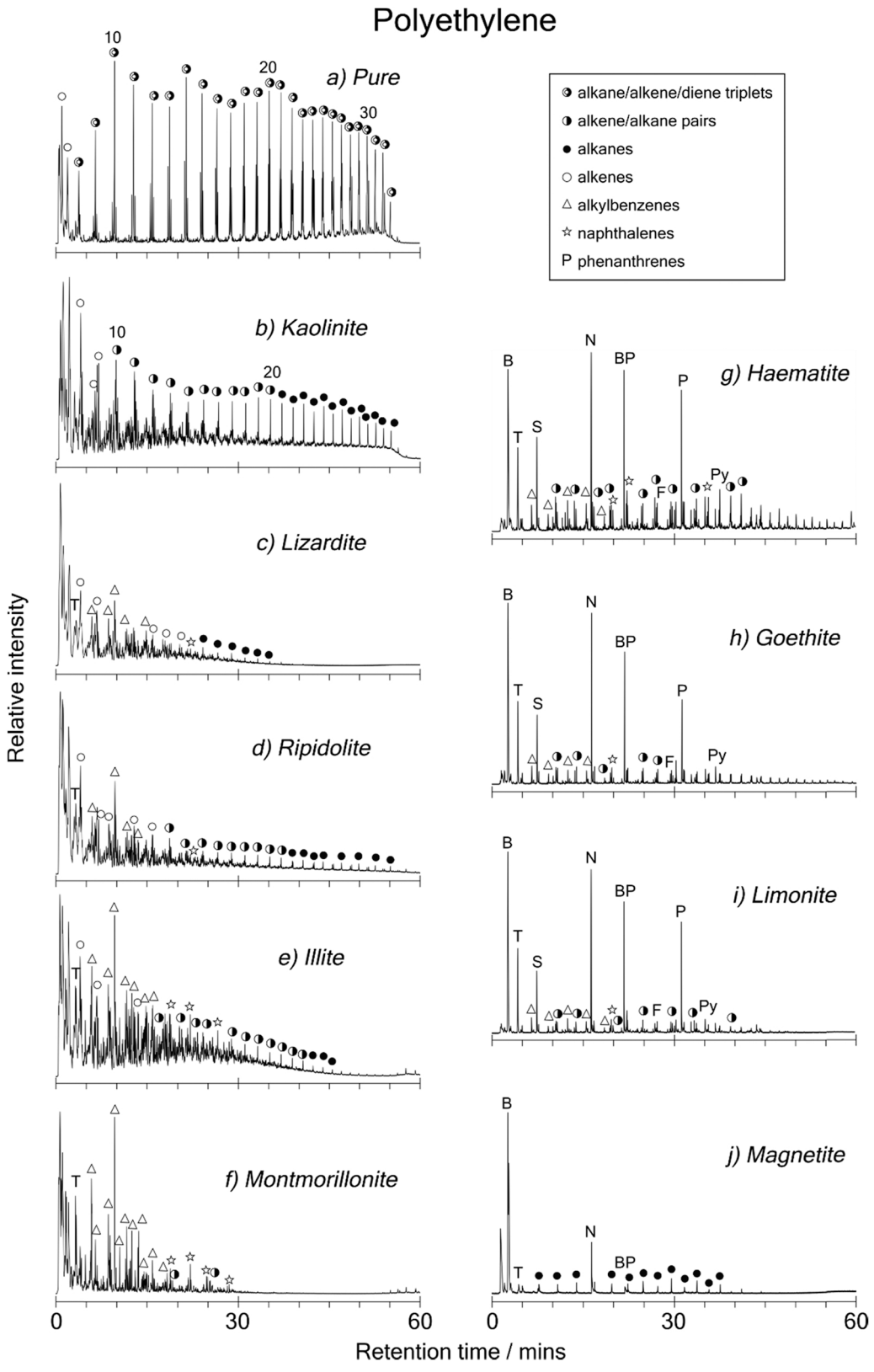

Fig. 1. Pyrolysis-GC-MS total ion chromatograms of (a) polyethylene and polyethylene (2% w/w) mixed with (b) kaolinite, (c) lizardite, (d) ripidolite, (e) illite, (f) montmorillonite, (g) haematite, (h) goethite, (i) limonite and (j) magnetite, all pyrolyzed at 650 °C. B: benzene, T: toluene, S: styrene, N: naphthalene, BP: biphenyl, F: fluorene, Py: pyrene.

is greatly reduced in intensity compared to the pure PE sample. The aromatic molecules, benzene, toluene, styrene, naphthalene, biphenyl and phenanthrene, dominate the TICs for PE mixed with haematite, goethite and limonite. Alkylbenzenes and alkylnaphthalenes were also detected. The TIC for PE mixed with magnetite, shown in Fig. 1j, shows an even more pronounced effect than the other iron oxides; it is dominated by benzene and naphthalene with only the alkane hydrocarbon component remaining.

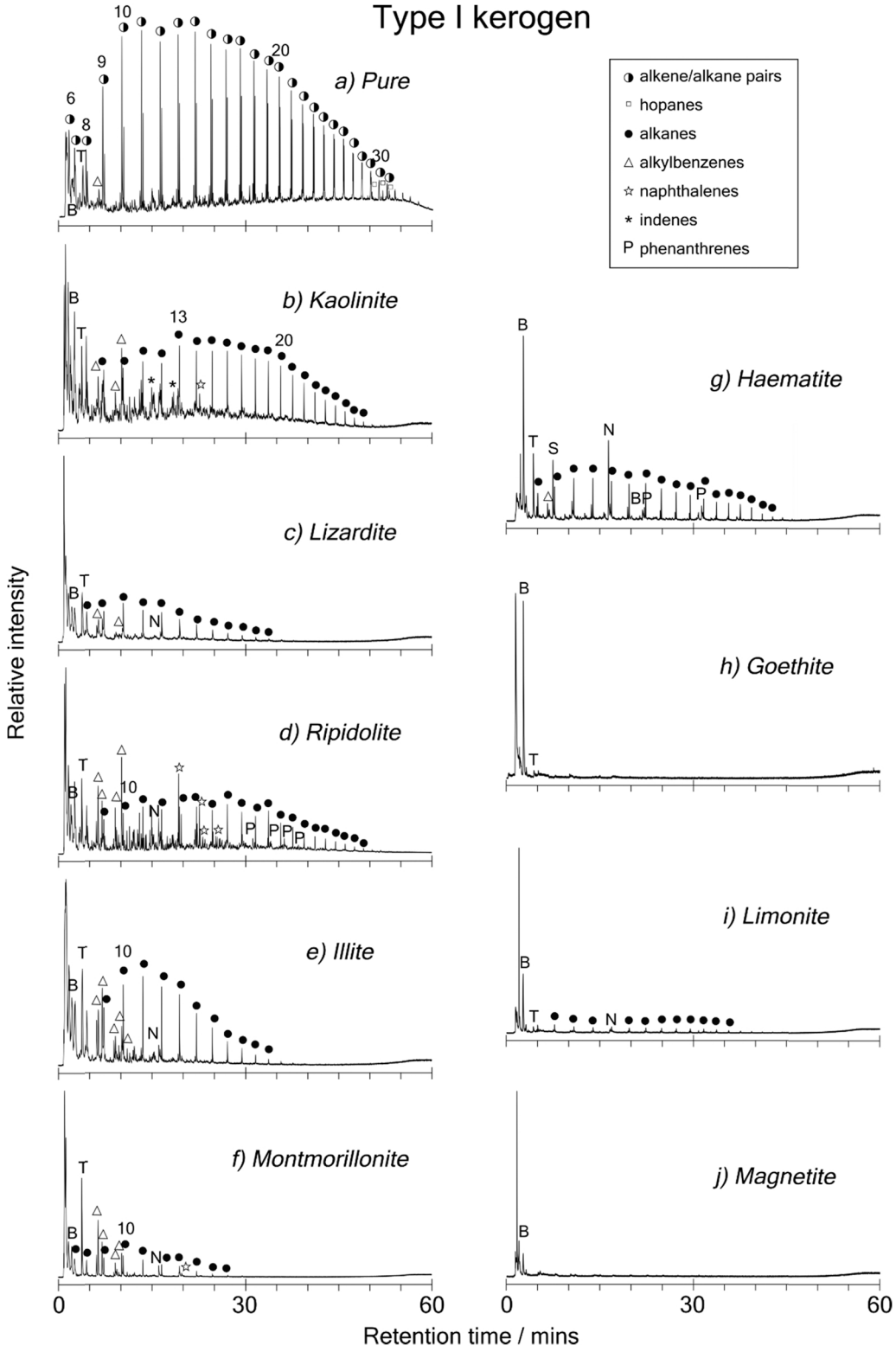

Fig. 2. Pyrolysis-GC-MS total ion chromatograms of (a) Type I kerogen (West Lothian shale) and Type I kerogen (2% w/w) mixed with (b) kaolinite, (c) lizardite, (d) ripidolite, (e) illite, (f) montmorillonite, (g) haematite, (h) goethite, (i) limonite and (j) magnetite, all pyrolyzed at 650 °C. B: benzene, T: toluene, S: styrene, N: naphthalene, BP: biphenyl.

3.2. Pyrolysis-GC-MS of Type I kerogen

The pyrolysis of the Type I kerogen (West Lothian shale), displayed in Fig. 2a, shows some similarities to the pyrolysis of pure PE. A series of *n*-alkene and *n*-alkane doublets were observed from C_6 to C_{31}, showing a maximum at C_{10} to C_{14} and then steadily decreasing in intensity. The alkene part was dominant, although the trend reversed at higher retention times, at approximately C_{22}. Benzene, toluene and xylene were also detected. At higher retention times, hopanes were also observed and are tentatively assigned to 17α(H)-trisnorhopane, 17α,21β(H)− 30-norhopane and 17α,21β(H)-hopane.

The effects of kaolinite, lizardite, ripidolite, illite and montmorillonite on the pyrolysis products of the Type I kerogen are shown in panels b to f of Fig. 2. A variety of different behaviours were observed when the Type I kerogen was mixed with phyllosilicates; in some cases most of the original signal was retained, while others were completely modified. Similar trends to the mixed PE samples were observed. In all cases the *n*-alkene/*n*-alkane doublet is reduced to the *n*-alkane component, the extent of which varies with the phyllosilicate, with kaolinite preserving the molecular weight distribution observed in the pure sample, and also displaying a relatively large intensity of *n*-alkanes, as shown in Fig. 2b. Ripidolite also showed similar behaviour, Fig. 2d. The other phyllosilicate minerals analysed all show reduced *n*-alkane series with up to C_{19} detected for lizardite and illite, and up to C_{16} detected for montmorillonite. All of the Type I kerogen samples mixed with phyllosilicates displayed in Fig. 2 show an increased number of aromatic molecules compared to the Type I kerogen analysed alone, with benzene, toluene, alkylbenzenes, naphthalene, alkylnaphthalenes and indenes all detected. Ripidolite shows a particularly large number of aromatic molecules which include phenanthrene and its methyl derivatives.

The effect of the iron oxides, haematite, goethite, limonite and magnetite, on the pyrolysis products of the Type I kerogen are shown in the panels g to j of Fig. 2. Iron oxides show a large modification to the original pyrolysis spectra, with only haematite and limonite retaining any of the original dominant pyrolysis products (alkane series). Aromatic molecules, particularly benzene, dominate the TICs for the Type I kerogen mixed with iron oxides. For the sample mixed with haematite, larger aromatic molecules, such as naphthalene, biphenyl and phenanthrene were also detected, Fig. 2g.

3.3. Pyrolysis-GC-MS of Type II kerogen

In contrast to pure samples of PE and the Type I kerogen, the Type II kerogen (Oxford Clay shale), shown in Fig. 3a, produces markedly different pyrolysis products and is characterised by a large number of aromatic compounds. Aromatic molecules detected include benzene and alkylbenzenes (toluene, xylene and its derivatives), naphthalene and alkylnaphthalenes, and indenes. Thiophene, benzothiophene and their methyl derivatives were also detected. A series of alkene and alkane doublets (C_{13} to C_{21}) were observed at a lower relative intensity at higher retention times.

The panels b to f of Fig. 3 show the effects of kaolinite, lizardite, ripidolite, illite and montmorillonite on the pyrolysis products of the Type II kerogen. Compared to the PE and Type I kerogen data, shown in Figs. 1 and 2 respectively, the data shown in Fig. 3 are quite different owing to the differences observed in the pure samples. Similar to the effects observed with PE and Type I kerogen, kaolinite mixed with Type II kerogen shows relatively few changes compared to the pure sample, although an increase in the relative intensity of indenes and alkylnaphthalenes, as well as the disappearance of the alkene/alkane doublets was observed. The pyrolysis products for the Type II kerogen mixed with ripidolite show very similar results to kaolinite, with larger peaks observed for alkylnaphthalenes. The TICs of lizardite and illite show similar results, dominated by alkylbenzenes and thiophenes. In contrast, the Type II kerogen mixed with montmorillonite, Fig. 3f, is dominated by higher molecular weight alkylbenzenes and alkylnaphthalenes, and larger polycyclic aromatic molecules such as fluorene and phenanthrenes.

Similarly to PE and the Type I kerogen, the iron oxides have a very pronounced effect on the pyrolysis products of the Type II kerogen, shown in panels g to j of Fig. 3. A large number of products were detected for the Type II kerogen mixed with haematite, Fig. 3g. These include the aromatic molecules, benzene, toluene, styrene, naphthalene, biphenyl, fluorene and phenanthrene, as well as some alkane peaks. Goethite and limonite have similar TICs with less pyrolysis products detected, and are dominated by benzene, toluene and naphthalene. Magnetite mixed with Type II kerogen, Fig. 3j, showed a few small alkane peaks as well as aromatic molecules; interestingly, benzonitrile was also detected.

4. Discussion

It can clearly be seen in the results presented above that different phyllosilicates and iron oxides have varying effects on the pyrolysis products of PE and the two kerogens analysed. The reactive effect of phyllosilicates is due to their large surface area and behaviour as strong Lewis acids [31,32]. The pyrolysis conditions induce thermal fission and generate organic free radicals. The organic free radicals can combine with hydrogen supplied from elsewhere within the fragmenting molecules or externally from other molecules or sources to produce stable products. The organic free radicals can also form unsaturated products if hydrogen availability is limited or hydrogen is abstracted and transferred to external sinks. The generation of unsaturated aromatic units, that were not observed in the pyrolysis products of unmodified starting materials, reveals that mineral assisted hydrogen removal is a likely mechanism for generating the aromatic pyrolysis products. To better visualise the effects that the minerals have, ternary diagrams for PE, Type I and Type II kerogens are shown in Fig. 4. The compounds detected were grouped into three families: aliphatic hydrocarbons, alkylbenzenes and alkylnaphthalenes. For PE and the Type I kerogen, increasing aromatisation was observed when the organic compounds were mixed with phyllosilicates, with a greater proportion of alkylbenzenes detected indicating that oxidative processes were taking place. Kaolinite, which has the least impact of the minerals analysed in this study, shows the largest amount of original pyrolysis products retained, although chain scission is observed, resulting in the absence of dienes in polyethylene, and the absence of alkenes in the Type I kerogen. This has been shown previously in the pyrolysis of Huadian oil shale kerogen mixed with kaolinite [17]. Kaolinite has also previously been shown to be a less active catalyst, attributed to its lower surface area and lower cation exchange capacity [22,33].

The greatest effects, using the phyllosilicates analysed in this study, were observed with the mixed montmorillonite samples which show large differences to the pyrolysis products of PE and kerogen, resulting in TICs that are almost unrecognisable when compared to the original. A large number of aromatic molecules were observed, particularly alkylbenzenes and naphthalenes, although a low intensity of the alkane background was still observed in the Type I kerogen mixed with montmorillonite. Previous studies have also observed a large amount of aromatisation and reduction in aliphatic hydrocarbons when organic compounds were pyrolysed with montmorillonite; this effect also increases as the proportion of clay to organic material increases [19,34]. Intermediate effects were observed for lizardite, ripidolite and illite which show varying stages of transformation between the extremes of kaolinite and montmorillonite. Comparing the ternary diagrams for the three organic compounds analysed, it can be seen that when PE and Type I kerogen are mixed with montmorillonite, the response is similar to pure Type II kerogen, indicating that interpretation issues could occur with Type I kerogen mistaken for Type II kerogen if it is analysed with certain phyllosilicates.

From Figs. 3 and 4 it can clearly be seen that the phyllosilicates have

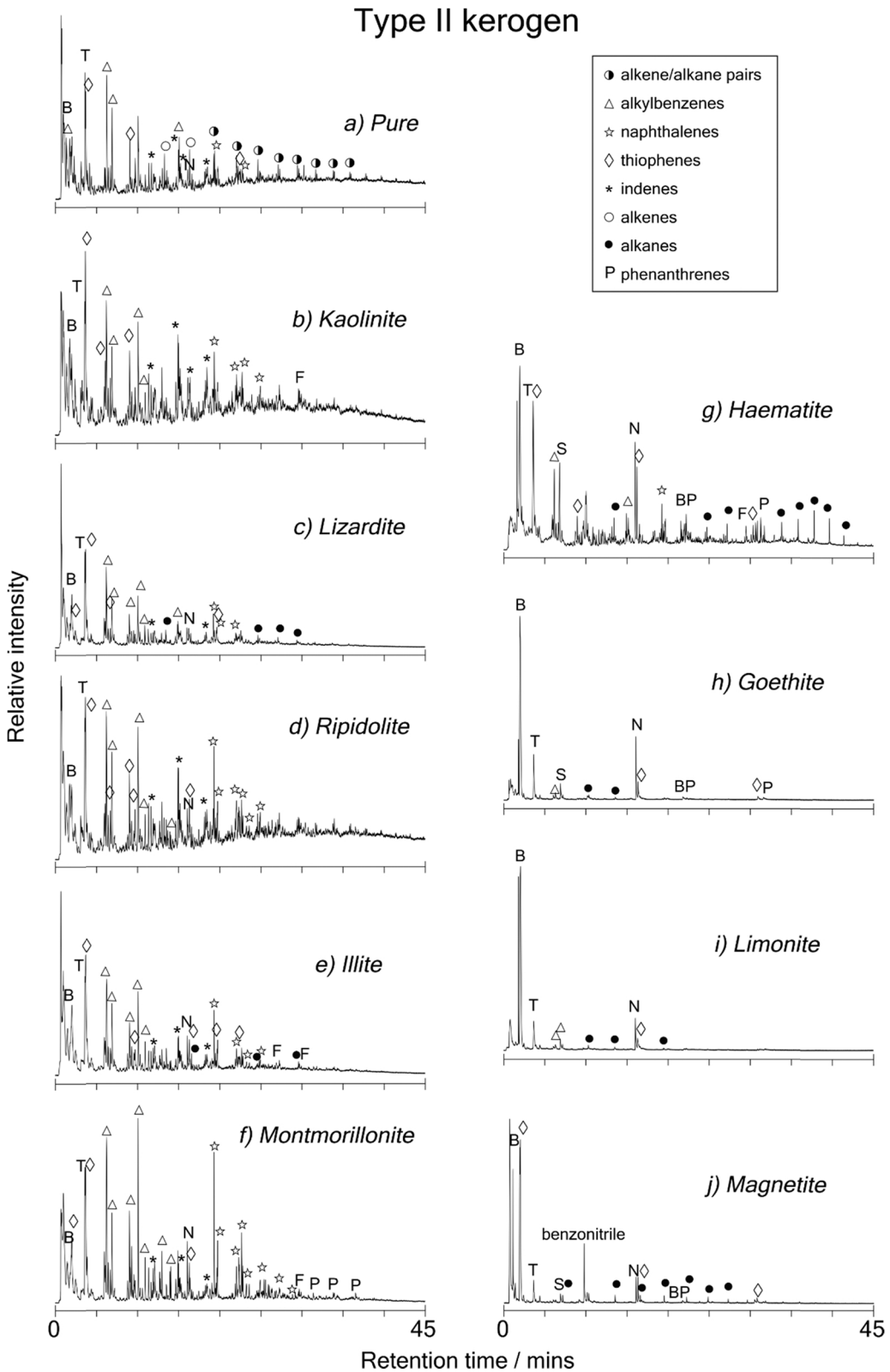

Fig. 3. Pyrolysis-GC-MS total ion chromatograms of (a) Type II kerogen (Oxford clay shale) and Type II kerogen (2% w/w) mixed with (b) kaolinite, (c) lizardite, (d) ripidolite, (e) illite, (f) montmorillonite, (g) haematite, (h) goethite, (i) limonite and (j) magnetite, all pyrolyzed at 650 °C. B: benzene, T: toluene, S: styrene, N: naphthalene, BP: biphenyl, F: fluorene.

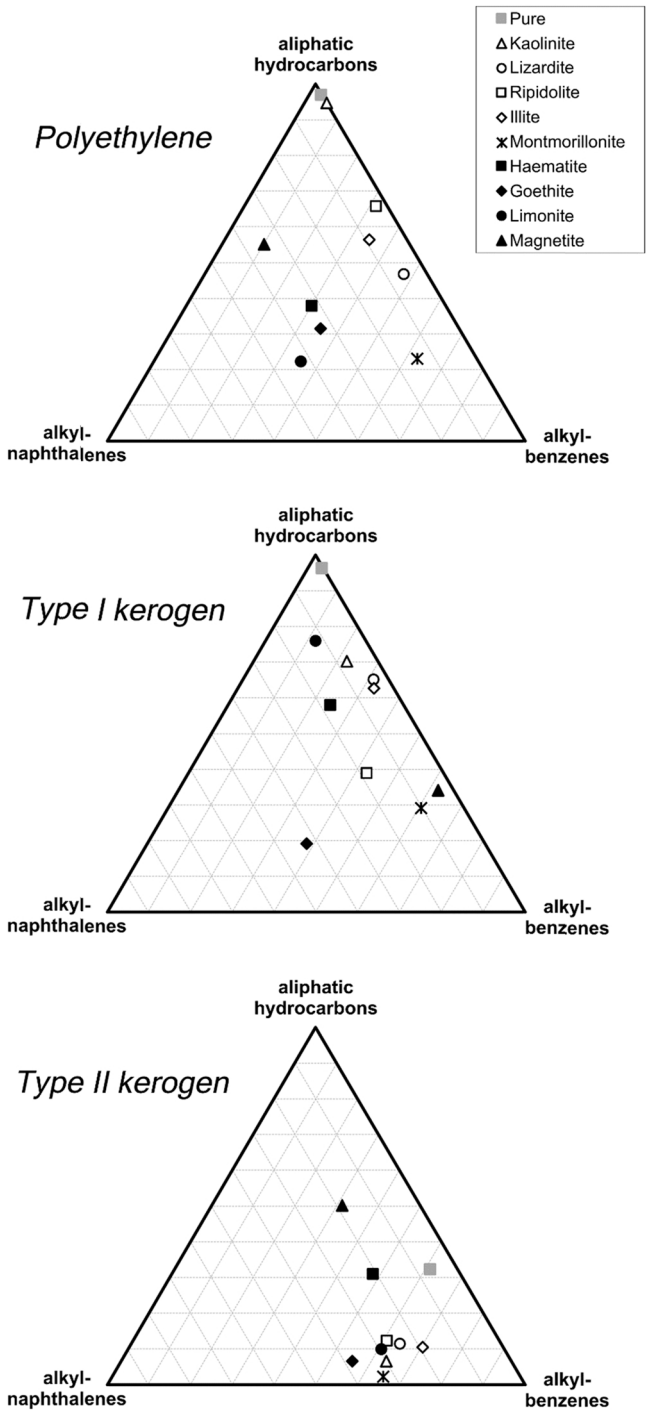

Fig. 4. Ternary diagrams of polyethylene, Type I and Type II kerogens illustrating the variation in the ratios of aliphatic hydrocarbons and one and two ring aromatics.

less of a distribution of effects on the Type II kerogen. Increased aromatisation to both alkylbenzenes and alkylnaphthalenes was observed, with hardly any aliphatic hydrocarbons remaining in the sample mixed with montmorillonite. The increase in the amount of naphthalenes and phenanthrenes when Type II kerogen is pyrolysed with montmorillonite, compared to pyrolysis alone, has been observed previously [27].

Fig. 4 also shows the effects of the iron oxides on the pyrolysis products of PE and Type I and II kerogens. The effects of the iron oxides is markedly different from the phyllosilicates with a greater proportion of alkylnaphthalenes detected for all the samples mixed with iron oxides. Goethite, limonite and magnetite decrease the signal to aromatic molecules such as benzene, toluene and naphthalene. This is evidence of oxidation, adsorption and/or polymerisation. The destruction of the original pyrolysis products makes it difficult to differentiate between the different organic materials when they are mixed with iron oxides.

5. Conclusions

Our data reveal that analytical pyrolysis in the presence of certain minerals has the potential to change the nature of the products and may cause incorrect interpretations of kerogen types. The mineralogy of samples should be considered when examining the analytical pyrolysates of whole rock samples of Type I and Type II kerogens. Polyethylene and Type I kerogen samples mainly produce aliphatic hydrocarbon pyrolysis products when they are pyrolysed by themselves, however in the presence of phyllosilicates and iron oxides, an increasing number of aromatic products are detected, similar to the pyrolysis products of Type II kerogen when it is pyrolyzed in pure form. Thermal processing of oil shale to generate petroleum liquids will also be influenced by the presence of minerals in a similar fashion.

Iron oxides dramatically affect the pyrolysis products of all the organic samples analysed with the resulting data being unrecognisable from the original pyrolysis spectra. Goethite, limonite and magnetite reduce the signal to a few aromatic compounds, including benzene, toluene and naphthalene. The phyllosilicates have differing impacts upon the pyrolysis products; kaolinite is the least active matrix with a large proportion of the original pyrolysis products detected. Lizardite, ripidolite, illite and montmorillonite show increasing amounts of aromatisation and a reduction in the number and intensity of aliphatic hydrocarbons.

Funding

This work was supported by funding from STFC (ST/S000615/1), UKSA (ST/V002732/1, ST/V006134/1) and The Leverhulme Trust (RPG-2018-012).

CRediT authorship contribution statement

Tara L. Salter: Investigation, Methodology, Formal analysis, Writing – original draft. **Jonathan S. Watson:** Conceptualization, Methodology, Writing – review & editing. **Mark A. Sephton:** Writing – review & editing, Supervision, Funding acquisition.

Declaration of Competing Interest

The authors declare that they have no known competing financial interests or personal relationships that could have appeared to influence the work reported in this paper.

Data availability

Data will be made available on request.

Acknowledgements

Thanks to Rob Lowther for the minerals from the ESE rock collection.

References

[1] V. Krevelen, Graphical-statistical method for the study of structure and reaction processes of coal, Fuel 29 (1950) 269–284.
[2] H. Dembicki, B. Horsfield, T.T.Y. Ho, Source rock evaluation by pyrolysis-gas chromatography, Am. Assoc. Pet. Geol. Bull. 67 (1983) 1094–1103, https://doi.org/10.1306/03B5B709-16D1-11D7-8645000102C1865D.
[3] D. van de Meent, S.C. Brown, R.P. Philp, B.R.T. Simoneit, Pyrolysis-high resolution gas chromatography and pyrolysis gas chromatography-mass spectrometry of

kerogens and kerogen precursors, Geochim. Cosmochim. Acta 44 (1980) 999–1013, https://doi.org/10.1016/0016-7037(80)90288-4.
[4] D. Lai, J.-H. Zhan, Y. Tian, S. Gao, G. Xu, Mechanism of kerogen pyrolysis in terms of chemical structure transformation, Fuel 199 (2017) 504–511, https://doi.org/10.1016/j.fuel.2017.03.013.
[5] S.R. Larter, A.G. Douglas, A pyrolysis-gas chromatographic method for kerogen typing, Phys. Chem. Earth 12 (1980) 579–583, https://doi.org/10.1016/0079-1946(79)90139-3.
[6] K. Øygard, S. Larter, J. Senftle, The control of maturity and kerogen type on quantitative analytical pyrolysis data, Org. Geochem. 13 (1988) 1153–1162, https://doi.org/10.1016/0146-6380(88)90301-4.
[7] R.W. Snyder, P.C. Painter, D.C. Cronauer, Development of FT-i.r. procedures for the characterization of oil shale, Fuel 62 (1983) 1205–1214, https://doi.org/10.1016/0016-2361(83)90065-0.
[8] A.K. Burnham, J.A. Happe, On the mechanism of kerogen pyrolysis, Fuel 63 (1984) 1353–1356, https://doi.org/10.1016/0016-2361(84)90336-3.
[9] P.R. Solomon, F.P. Miknis, Use of Fourier Transform infrared spectroscopy for determining oil shale properties, Fuel 59 (1980) 893–896, https://doi.org/10.1016/0016-2361(80)90040-X.
[10] E. Tannenbaum, B.J. Huizinga, I.R. Kaplan, Role of minerals in thermal alteration of organic matter–II: a material balance, Am. Assoc. Pet. Geol. Bull. 70 (1986) 1156–1165, https://doi.org/10.1306/94886A92-1704-11D7-8645000102C1865D.
[11] B.J. Huizinga, E. Tannenbaum, I.R. Kaplan, The role of minerals in the thermal alteration of organic matter—III. Generation of bitumen in laboratory experiments, Org. Geochem. 11 (1987) 591–604, https://doi.org/10.1016/0146-6380(87)90012-X.
[12] H. Dembicki, The effects of the mineral matrix on the determination of kinetic parameters using modified Rock Eval pyrolysis, Org. Geochem. 18 (1992) 531–539, https://doi.org/10.1016/0146-6380(92)90116-F.
[13] W.D. Johns, Clay mineral catalysis and petroleum generation, Annu. Rev. Earth Planet. Sci. 7 (1979) 183–198, https://doi.org/10.1146/annurev.ea.07.050179.001151.
[14] B.S. Greensfelder, H.H. Voge, G.M. Good, Catalytic and thermal cracking of pure hydrocarbons: mechanisms of reaction, Ind. Eng. Chem. 41 (1949) 2573–2584, https://doi.org/10.1021/ie50479a043.
[15] K.G.J. Nierop, P.F. Van Bergen, Clay and ammonium catalyzed reactions of alkanols, alkanoic acids and esters under flash pyrolytic conditions, J. Anal. Appl. Pyrolysis 63 (2002) 197–208, https://doi.org/10.1016/S0165-2370(01)00154-1.
[16] B. Spiro, Effects of minerals on Rock Eval pyrolysis of kerogen, J. Therm. Anal. 37 (1991) 1513–1522, https://doi.org/10.1007/BF01913484.
[17] M. Hu, Z. Cheng, M. Zhang, M. Liu, L. Song, Y. Zhang, J. Li, Effect of calcite, kaolinite, gypsum, and montmorillonite on huadian oil shale Kerogen pyrolysis, Energy Fuels 28 (2014) 1860–1867, https://doi.org/10.1021/ef4024417.
[18] C. Pan, L. Jiang, J. Liu, S. Zhang, G. Zhu, The effects of calcite and montmorillonite on oil cracking in confined pyrolysis experiments, Org. Geochem. 41 (2010) 611–626, https://doi.org/10.1016/j.orggeochem.2010.04.011.
[19] P. Faure, L. Schlepp, L. Mansuy-Huault, M. Elie, E. Jardé, M. Pelletier, Aromatization of organic matter induced by the presence of clays during flash pyrolysis-gas chromatography–mass spectrometry (PyGC–MS): a major analytical artifact, J. Anal. Appl. Pyrolysis 75 (2006) 1–10, https://doi.org/10.1016/J.JAAP.2005.02.004.
[20] J. Espitalie, M. Madec, B. Tissot, Role of mineral matrix in kerogen pyrolysis: influence on petroleum generation and migration, Am. Assoc. Pet. Geol. Bull. 64 (1980) 59–66, https://doi.org/10.1306/2F918928-16CE-11D7-8645000102C1865D.
[21] R. Zafar, J.S. Watson, Adsorption of tetradecanoic acid on kaolinite minerals: using flash pyrolysis to characterise the catalytic efficiency of clay mineral adsorbed fatty acids, Chem. Geol. 471 (2017) 111–118, https://doi.org/10.1016/J.CHEMGEO.2017.09.020.
[22] Z. Wei, J. Michael Moldowan, J. Dahl, T.P. Goldstein, D.M. Jarvie, The catalytic effects of minerals on the formation of diamondoids from kerogen macromolecules, Org. Geochem. 37 (2006) 1421–1436, https://doi.org/10.1016/J.ORGGEOCHEM.2006.07.006.
[23] H. Bu, P. Yuan, H. Liu, D. Liu, J. Liu, H. He, J. Zhou, H. Song, Z. Li, Effects of complexation between organic matter (OM) and clay mineral on OM pyrolysis, Geochim. Cosmochim. Acta 212 (2017) 1–15, https://doi.org/10.1016/J.GCA.2017.04.045.
[24] S. Li, S. Guo, X. Tan, Characteristics and kinetics of catalytic degradation of immature kerogen in the presence of mineral and salt, Org. Geochem. 29 (1998) 1431–1439, https://doi.org/10.1016/S0146-6380(98)00154-5.
[25] X. Ma, G. Zheng, W. Sajjad, W. Xu, Q. Fan, J. Zheng, Y. Xia, Influence of minerals and iron on natural gases generation during pyrolysis of type-III kerogen, Mar. Pet. Geol. 89 (2018) 216–224, https://doi.org/10.1016/J.MARPETGEO.2017.01.012.
[26] M. Hetényi, Simulated thermal maturation of type I and III kerogens in the presence, and absence, of calcite and montmorillonite, Org. Geochem. 23 (1995) 121–127, https://doi.org/10.1016/0146-6380(94)00120-P.
[27] S.T. Lu, I.R. Kaplan, Pyrolysis of kerogens in the absence and presence of montmorillonite—II. Aromatic hydrocarbons generated at 200 and 300°C, Org. Geochem. 14 (1989) 501–510, https://doi.org/10.1016/0146-6380(89)90030-2.
[28] C. Pan, A. Geng, N. Zhong, J. Liu, L. Yu, Kerogen pyrolysis in the presence and absence of water and minerals: Amounts and compositions of bitumen and liquid hydrocarbons, Fuel 88 (2009) 909–919, https://doi.org/10.1016/j.fuel.2008.11.024.
[29] L. He, H. Hui, S. Li, W. Lin, Production of light aromatic hydrocarbons by catalytic cracking of coal pyrolysis vapors over natural iron ores, Fuel 216 (2018) 227–232, https://doi.org/10.1016/J.FUEL.2017.12.005.
[30] L. He, S. Li, W. Lin, Catalytic cracking of pyrolytic vapors of low-rank coal over limonite ore, Energy Fuels 30 (2016) 6984–6990, https://doi.org/10.1021/ACS.ENERGYFUELS.6B01182.
[31] B. Horsfield, A.G. Douglas, The influence of minerals on the pyrolysis of kerogens, Geochim. Cosmochim. Acta 44 (1980) 1119–1131, https://doi.org/10.1016/0016-7037(80)90066-6.
[32] J. Espitalié, K. Senga Makadi, J. Trichet, Role of the mineral matrix during kerogen pyrolysis, Org. Geochem. 6 (1984) 365–382, https://doi.org/10.1016/0146-6380(84)90059-7.
[33] Z. Lu, X. Zhao, Z. Liu, Q. Liu, Mutual influences between organic matter and minerals during oil shale pyrolysis, Energy Fuels 33 (2019) 1850–1858, https://doi.org/10.1021/acs.energyfuels.8b03703.
[34] P. Faure, L. Jeanneau, F. Lannuzel, Analysis of organic matter by flash pyrolysis-gas chromatography–mass spectrometry in the presence of Na-smectite: When clay minerals lead to identical molecular signature, Org. Geochem. 37 (2006) 1900–1912, https://doi.org/10.1016/J.ORGGEOCHEM.2006.09.008.
[35] J. Espitalié, J.L. Laporte, M. Madec, F. Marquis, P. Leplat, J. Paulet, A. Boutefeu, Méthode rapide de caractérisation des roches mètres, de leur potentiel pétrolier et de leur degré d'évolution, Rev. l'Inst. Fr. Pét. 32 (1977) 23–42, https://doi.org/10.2516/ogst:1977002.